APPENDIX B

"CHEMICAL AND PHYSICAL PROCESSES IN COUNTERCURRENT FIXED-BED COAL GASIFICATION"

Paper Submitted to the 23rd International Symposium of the Combustion Institute, 1990

Submitted to the 23rd International Symposium on Combustion

Subject Matter: Coal Combustion, Combustion in Practical Systems, Modeling and Simulation

CHEMICAL AND PHYSICAL PROCESSES IN COUNTERCURRENT FIXED-BED COAL GASIFICATION

M. L. Hobbs, P. T. Radulovic and L. D. Smoot§
Advanced Combustion Engineering Research Center
Brigham Young University
Provo, Utah 84602
(801) 378-4326

Word Count:

Text:	3400
References:	675
Acknowledgement:	100
Figures:	1400
Tables:	200
Total:	**5000**

(Excluding References and Acknowledgement)

§ The author to whom the correspondence should be directed

CHEMICAL AND PHYSICAL PROCESSES IN COUNTERCURRENT FIXED-BED COAL GASIFICATION

M. L. Hobbs, P. T. Radulovic and L. D. Smoot
Advanced Combustion Engineering Research Center
Brigham Young University, Provo, Utah 84602

The objective of this paper is to investigate and model chemical and physical processes in slowly moving beds (i.e. fixed beds) of gasifying coal. A one-dimensional model of countercurrent fixed-bed gasification has been developed and results have been compared to experimental data obtained from a large scale gasifier. The steady-state model considers separate gas and solid temperatures, partial equilibrium in the gas phase, variable bed void fraction, coal drying, devolatilization based on chemical functional group composition, oxidation and gasification of residual char with an ash layer, and axially variable solid and gas flow rates. An accurate initial estimate of the effluent composition and temperature from a two-zone, partial equilibrium model has been found essential for this highly nonlinear problem. Predictions and comparisons to experimental data include effluent gas compositions and temperatures, temperature profiles, and axial pressure variation. Additional predictions with comparison to limited data include carbon conversion, variable particle size, and species concentration profiles. The relative importance of char oxidation resistances to bulk film diffusion, ash diffusion, and chemical reaction are identified. For the cases examined, chemical resistance dominates in the cool regions at the bottom and top of the reactor while ash diffusion resistance competes with chemical resistance through most of the reactor. The importance of adequate treatment of devolatilization, gas phase chemistry, and variable bed void fraction is identified.

Introduction

Commercial coal gasification has been used to obtain synthetic fuel as well as petrochemical feedstocks for over 200 years. The most important commercial gasification process is fixed-bed gasification. Eighty-nine percent of gasified coal is by fixed-bed, ten percent is by entrained-bed, and only one percent is by fluidized-bed.

A demonstration, Wellman-Galusha fixed-bed gasifier[1] is shown schematically in Fig. 1. Coal is fed to the top of the reactor from two coal lock hoppers and moves downward under gravity, countercurrent to the rising gas stream. The dry ash is removed at the bottom of the reactor. The influent or blast gas is composed of air saturated with steam. The steam-to-air ratio is used to control the ash temperature.

Figure 1 shows the reactor divided into four overlapping zones: i) drying, ii) devolatilization, iii) gasification, and iv) combustion. As the coal slowly descends, the hot gases produced in the gasification and combustion zones exchange energy with the cool solid. Water and

volatile matter are released when the solid reaches a sufficiently high temperature. After drying and devolatilization, the char enters the gasification zone where carbon reacts with steam, carbon dioxide and hydrogen. Endothermic reactions in this section produce carbon monoxide and hydrogen. The slightly exothermic reaction of hydrogen with carbon produces methane. Differentiation between the "gasification zone" and "combustion zone" can be determined by the presence of free oxygen. Combustion and gasification reactions can occur simultaneously in the "combustion zone". Combustible gases such as carbon monoxide or hydrogen may react with oxygen. Solid residence time in the drying, gasification and oxidation zones may be on the order of several hours. Residence time in the ash layer may be even higher depending on the thickness of this zone. The large solid residence times indicate significant settling resulting in variable axial velocities. Gas residence times are on the order of seconds.

Amundson and Arri[2] applied a detailed char model to a countercurrent reactor. Soon afterward, Yoon et al.[3], Desai and Wen[4], and Stillman[5] presented detailed models of a fixed-bed gasifier. Even though the model of Yoon et al. in 1978 was rather sophisticated, simpler global models continued to be developed.[6,7,8] Cho and Joseph[9] extended Yoon's model to include unequal gas-solid temperatures. Yoon's model was further extended by Kim and Joseph[10] to account for transient affects. Yu and Denn[11] extended Yoon's model to two space dimensions. More recent models include the one-dimensional, steady-state model of Earl and Islam[12], and the two-dimensional, transient models of Thorsness and Kang[13] and Bhattacharya et al.[14]. Khanna and Seinfeld[15] show recent advances in catalytic fixed-bed models which have many of the features of coal gasification/combustion fixed-bed models.

No major advancements have been reported in comprehensive fixed-bed gasifier or combustor modeling in the past few years. An assessment of fixed-bed models indicates common assumptions such as equal gas/solid temperatures, axially uniform gas/solid phase plug flow, uniform bed porosity, instantaneous devolatilization (with volatile yield from proximate analysis and composition assumed to be constant), char oxidation parameters from small particle data, and little or no gas phase chemistry. The model presented in this paper relaxes all of these assumptions.

Fixed-bed Model

Model Foundations

The foundation of the model is the conservation equations for mass and energy. The source terms in the continuity and energy equations are described by various physical and chemical submodels. Input parameters are reactor dimensions, operating conditions, inlet solid and gas temperature, pressure, concentrations, and flow rates and wall temperature. Calculated quantities include axial variation in gas temperature, solids temperature, pressure, species concentration, gas

flow rate, solid flow rate and wall heat loss. Plug flow is assumed in both the solid and gas phase with variable axial velocities. Gas phase pressure drop is calculated with the Ergun equation[16] for packed beds. An effective heat transfer coefficient is used for heat loss to the wall, including both stagnant and dynamic contributions as well as conduction and diffusive radiation. Large coal particle devolatilization occurs simultaneously with char oxidation and gasification. A shell progressive shrinking core model[13] describes oxidation and gasification. Equilibrium is used to calculate gas concentrations and temperatures. Turbulence is not treated formally in the slowly moving bed with low gas velocities, but is included implicitly through model correlations such as the effective heat transfer coefficient.

Table 1 summarizes general assumptions, conservation equations and boundary conditions for the one-dimensional, fixed-bed model. Reaction source terms represent coal drying and devolatilization, and char oxidation and gasification. These chemical and physical processes are shown in Fig. 2. Drying is assumed to be water vapor diffusion-limited. Devolatilization is described by assuming that the organic portion of the coal particle is composed of various functional groups: carboxyl, hydroxyl, ether, nitrogen, etc. A detailed functional group model (FG model) has been used to describe the devolatilization process[17,18,19,20]. The kinetics for evolution of each functional group are taken to be independent of the type of coal. Oxidation and gasification reactions consume the nonvolatile portion of the dry, ash-free coal. Three gasification reactants are considered: steam, carbon dioxide, and hydrogen. Volatile functional groups can competitively evolve as light gases or tar. Tar is treated as a single species that has a variable composition dependent on the location in the reactor, and can be treated in full or partial chemical equilibrium or kinetically. Gas temperature is determined by assuming all gas species to be in thermal equilibrium even though chemical equilibrium may not exist. Gas phase composition is determined by Gibbs free energy minimization. Locally varying solid temperature is determined from enthalpy and the elemental composition of the coal. All gas phase transport properties (conductivity, viscosity, diffusivity, etc.) are considered to be functions of temperature and composition.

An accurate initial estimate of the effluent composition and temperature was essential for an effective solution. With effluent conditions specified, the initial value solver LSODE[21] provides rapid, robust convergence.

Conservation Equations

Table 1 summarized the gas and solid overall continuity, gas and solid energy equations, and gas and solid species or elemental continuity equations. The constitutive relations for solid flow have been proposed only recently and no solution for these equations has been attempted.

Drying

The chemical submodels are composed of coal drying and devolatilization, char oxidation and gasification, and gas phase chemistry. Diffusion-limited vaporization of moisture from the coal particle is described by[22]:

$$r_w = k_{wm}\left(\rho_{wp} - \rho_{wg}\right) \qquad (1)$$

where k_{wm}, ρ_{wp} and ρ_{wg} represent the moisture mass transfer coefficient, surface moisture concentration and bulk water concentrations respectively. Blowing or transpiration effects influence the rates by approximately 5% for large particles, and while included in the model, have been neglected for the calculations herein.

Devolatilization

Coal devolatilization rates can be described by consumption of solid or by production of light gas and tar:

$$r_i = \rho^{\circ}_{sm}\left(1-\varepsilon^{\circ}\right)\left(1-\Omega^{\circ}_{ash}-\Omega^{\circ}_{moisture}\right)\frac{d\omega_{i,\,(char,\,tar,\,or\,gas)}}{dt} \qquad (2)$$

where ρ°_{sm} is measured apparent density of the feed coal, ε° is the bed void fraction of the feed coal, Ω°_{ash} and $\Omega^{\circ}_{moisture}$ are the proximate ash and moisture fractions of the feed coal, and $\omega_{i,(char,\ tar,\ or\ gas)}$ is the weight fraction of the i^{th} functional group in the char, tar, or gas. The time derivatives in Eq. (2) were calculated by assuming that light gases do not evolve from the gaseous tar:

$$\frac{d\omega_{i,gas}}{dt} = \left(1-x^{\circ}+x\right)k_i Y_i \text{ and } \frac{d\omega_{i,tar}}{dt} = k_x x Y_i \qquad (3)$$

$$\frac{d\omega_{i,char}}{dt} = -\frac{d\omega_{i,gas}}{dt} - \frac{d\omega_{i,tar}}{dt} \qquad (4)$$

$\omega_{i,gas}$, $\omega_{i,tar}$, and $\omega_{i,char}$ represent fractional amounts of a particular functional group component that has evolved as light gas, tar or is remaining in the solid. Normally distributed Arrhenius rate coefficients for 19 functional groups and tar, k_i and k_x, where obtained from Solomon et al.[20] for the organic functional groups depicted in Fig. 2. The X and Y values represent the two-dimensional description of coal[18]. The Y dimension is divided into fractions according to the chemical composition of the coal. The initial fraction of a particular functional group component is represented by Y_i°, and the sum of Y_i°'s equals 1. The evolution of each functional group into the gas is represented by the first order decay of the Y dimension, $\frac{dY_i}{dt} = -k_i Y_i$. The X dimension

represents non-tar-forming char, tar-forming-char, and tar. The evolution of tar is represented to be the first order decay of the X dimension, $\frac{dx}{dt} = -k_x x$. The potential tar forming fraction, x^o, was adjusted herein to match experimentally determined tar yields, though it can also be predicted.

Oxidation and Gasification

A shrinking core model with a developing ash layer, commonly referred to as the shell progressive char oxidation model[13], is used for the calculations presented in this paper. The reaction rate for a single coal particle can be derived as[23]:

$$r_p = \frac{A_p \upsilon_s M_p C_{ig}}{\left(\frac{1}{k_r \zeta} + \frac{1}{k_m} + \frac{1}{k_{ash}}\right)} \qquad (5)$$

where the resistances in the denominator represent surface reaction, molecular diffusion through the gaseous film and diffusion through the ash layer. Equation (5) neglects the effects of diffusion-induced convective transport and assumes that the reactions are first order in oxidizer concentration. Quantities A_p, ν_s, M_p, C_{ig}, k_r, ζ, k_m, and k_{ash} represent the external surface area of the particle, the stoichiometric coefficient to identify the number of moles of product gas per mole of oxidant, char molecular weight, molar concentration of oxidizer or gasification agent in the bulk gas phase, Arrhenius chemical reaction rate constant, particle area factor to account for internal surface burning, bulk mass transfer coefficient, and ash layer mass transfer coefficient, respectively.

The last resistance in the denominator of Eq. 5 can be determined using an effective mass transfer coefficient[13]:

$$\frac{1}{k_{ash}} = \frac{(1-F)d}{2D_{eff}} \qquad (6)$$

where F, d, and D_{eff} represent the fraction of original carbon, coal particle diameter, and effective diffusivity, respectively. Walker et al.[24] and Laurendeau[25] discuss methods for calculating effective diffusivities. Park and Edgar[26] show the effect of a developing ash layer on the burning rate of a core sample of coal. The core burning rate can be predicted by using an effective diffusivity based on the molecular diffusivity multiplied by a constant ($D_{eff} = \phi D_m$). The constant, ϕ, is based on the porosity of the developing ash layer. Thorsness and Kang [13] have used 0.35 for ϕ which is based on the ash porosity. Wang and Wen[27] have measured porosity of a fire clay ash which varied from 0.44 to 0.75. Laurendeau[25] shows that ϕ can be estimated by the ash porosity divided by two. The value two is an estimate of the tortuosity squared. Since ϕ is a function of ash porosity and developing pore structure, ϕ was chosen as 0.18 for this study.

The single particle model can be related to the bed by use of the particle number density and unreacted core particle surface area. The particle diameter, unreacted core diameter and number density were obtained by mass balance, assuming spherical particles:

$$d = \left[(1-\Omega^{o}_{ash})d_u^3 + \Omega^{o}_{ash}d_o^3\right]^{1/3} \tag{7}$$

$$d_u = F^{1/3}d_o \tag{8}$$

$$n = \frac{6(1-\varepsilon)}{\pi d^3} \tag{9}$$

where the subscripts o and u represent initial and unreacted core respectively. A simple swelling model has been included to represent particle swelling during devolatilization:

$$d = d^{o}\left[1+\gamma\left(\frac{V}{V_\infty}\right)\right] \tag{10}$$

where γ, V, and V_∞ represent the swelling factor (chosen as 0.25 for Jetson bituminous coal with a free swelling index of 2), volatiles content, and the ultimate volatiles content, respectively.

Heat and Mass Transfer Coefficients

The heat transfer coefficient for particle to gas heat transfer was obtained following Gupta and Thodos[28]:

$$h_{sg} = \frac{2.06RT}{\varepsilon P}\mathrm{Re}^{-0.575}\mathrm{Pr}^{-0.667} \tag{11}$$

This correlation is based on evaporation of water from a packed-bed of spheres. For a reacting bed of particles, Cho[29] indicates the solid to gas heat transfer coefficient to be smaller than that predicted by Eq. (14). The mass transfer coefficient used in Eq. (5) is also obtained from Gupta and Thodos[28]:

$$k_m = \frac{2.06G}{\varepsilon\rho_g}\mathrm{Re}^{-0.575}\mathrm{Sc}^{-0.667} \tag{12}$$

where G is the superficial mass velocity of the flowing gas.

The bed-to-wall heat transfer coefficient for the gas and particle phase can be determined from the overall bed-to-wall effective heat transfer coefficient which is discussed by Froment and Bischoff[30]:

$$h_w = \frac{2.44k_r^{o}}{D^{1/3}} + \frac{0.0333k_g\mathrm{PrRe}}{d} \tag{13}$$

where k_r^{o}, D, and k_g represent the static contribution of the effective radial conductivity, reactor diameter, and gas thermal conductivity respectively. The static contribution of the effective radial conductivity includes diffusive void-to-void radiation and solid diffusive radiation terms. More information regarding heat and mass transfer correlations for packed-beds can be found in Froment and Bischoff[30], Kunii and Smith[31], and Solomon et al.[32].

Chapman-Enskog theory has been used to calculate multicomponent gas mixture viscosity and diffusivity[33]. The JANAF tables were used to calculate gas-phase enthalpy, entropy, and heat capacity[34]. Solid enthalpy and heat capacities were determined using Merrick's correlations[35]. Most fixed-bed models in the literature assume that the solid and gas properties (i. e. conductivity, heat capacity, viscosity, molecular weight) are not functions of pressure, temperature or composition. However, it was found that gas properties are strong functions of temperature with maximum values occurring near the temperature peak .

Experimental Data

Detailed experimental data were sought for model evaluation. Unfortunately, only limited detailed data exist, at least in the open literature. There are no published data available for separate gas and solids temperatures or gas composition in the bed. The most extensive set of fixed-bed data that includes limited profile data was compiled by Thimsen et al.[1]. Data for seventeen coals (bituminous, subbituminous, and lignite), peat, and coke were reported. The data include gasifier operation data, coal data, tar and water yield, ash and dust data, and gas composition. Some profile data for temperature and pressure were also reported. The most comprehensive set of data for gasification of Jetson high-volatile-B bituminous coal was selected for use in this study. The general schematic for this reactor and operating conditions were presented in Fig. 1.

Data and Model Comparisons

Compositions and Temperatures

The measured and predicted effluent gas composition and temperature are compared in Fig. 3a. The agreement is acceptable, considering that the predictions did not account for the processes which occur in the space above the coal bed. The measured and predicted influent gas composition and temperature are compared in Fig. 3b. Again the agreement is reasonable. The measured and predicted carbon conversion near the grate are also in close agreement.

The measured and predicted temperature profiles are presented in Fig. 4a. The jump near the bottom of the gasifier is caused by heterogeneous oxidation. The drop near the reactor top is caused by devolatilization. The oxidation jump is evident both in the measured and in the predicted profiles. The predicted maximum temperature is high compared to measurements. However, it was reported[1] that the temperature probe was retracted from the reactor if any thermocouple junction read 1589 K (the temperature limit of the materials of the probe) which did not allow peak temperature measurements in the combustion zone of most fuels. The predicted devolatilization temperature drop seems large and steep, although there are no measured data at this location for comparison. The difference between the gas and solids temperatures is expected to be greater in this region. The predicted carbon conversion profile is shown in Fig. 4b. The overall shape

seems qualitatively correct, but there are no measured profile data for comparison. The devolatilization jump is probably too high and too steep since axial mass transport of volatile matter was neglected. Figure 4b also shows the change in particle diameter, unreacted core diameter, and ash layer thickness throughout the reactor.

The predicted concentration profiles for major and minor species are shown in Fig. 5 assuming local gaseous chemical equilibrium. The blast gas is composed of air and steam. The oxidation of carbon was assumed to form CO at the surface of the char. The CO reacts in the gas phase to produce CO_2. The CO_2 peak occurs concurrently with the temperature peak. After oxygen depletion, the CO_2 reacts with the char to form CO, which begins to increase after the peak. Any CO or H_2 produced by steam gasification in the presence of oxygen was further oxidized in the gas phase to form CO_2 and H_2O. These highly exothermic reactions can partially explain the high predicted temperature peak. Assuming partial equilibrium in the gas phase may improve the temperature predictions.

Several minor species are produced in equilibrium in the reactor which decay to low values before reaching the reactor exit. These include NO, OH, and SO_2 which form in the high temperature and oxygen-rich environment near the bottom of the reactor. The devolatilization zone shows an increase in CO, H_2, and CH_4. In fact, all the CH_4 is attributed to devolatilization reactions. Normally, CH_4 is not produced at low pressures typical of this gasifier. The concentrations of N_2, CO_2 and H_2O decrease in the devolatilization zone of the reactor due to dilution effects.

Figure 6 shows the predicted carbon consumption by char oxidation and gasification reactions. The temperature peak occurs just before all oxygen is consumed in the oxidation reaction. Before oxidation is complete, steam and CO_2 gasification reactions begin. Hydrogen reacts with oxygen in the oxidation zone to form steam. Figure 6 also shows chemical, ash, and film resistances. Chemical resistance dominates at the top and bottom of the reactor where the temperatures are low. After the initial coal heats up to high temperatures, film resistance dominates at the top of the reactor. The ash resistance here is near zero since the ash layer is very small. Once the ash layer is sufficiently thick, ash diffusion competes with chemical reaction resistance. This competition occurs throughout most of the reactor. Although confidence in mass transfer coefficients is greater than chemical reaction coefficients, ash porosity is unknown throughout the reactor, and the effective ash diffusivity is difficult to predict. The effective diffusivity was assumed to be equal to the molecular diffusivity multiplied by a constant related to typical ash porosity for these predictions.

Pressure Drop

Figure 7 compares measured and predicted variation in pressure with different assumptions regarding the bed void fraction. The bed void fraction was measured at the top (coal feed void fraction is 0.31) and bottom of the gasifier (ash zone void fraction is 0.64). A constant bed void fraction (average of the coal feed and ash zone void fraction, 0.47) and linearly varying bed void fraction were used in the calculation. Qualitative agreement was obtained between the predicted and measured pressure variation for both assumptions. The pressure drop is smaller in the ash zone due to lower gas mass flow rate and larger void fraction possibly caused by ash clinkers. Quantitative agreement was obtained by varying the bed void fraction linearly. The pressure profile is a sensitive indication that both void fraction and gas flow rate are predicted correctly. Accurate values of void fraction and gas flow rate are essential for quantitative profile predictions.

Conclusions

The importance of treating various chemical and physical processes in fixed-bed gasifiers with sufficient detail has been addressed with emphasis on coal devolatilization, char oxidation, gas phase chemistry, and bed void fraction. Calculations have shown that devolatilization in fixed-bed reactors is not an instantaneous process but is an intimate part of the overall fixed-bed process. Similarly, oxidation and gasification do not occur in separate zones, but simultaneously in certain regions of the reactor bed. Competition between endothermic gasification reactions and exothermic oxidation is evident in broad predicted and measured temperature peaks. Detailed gas phase chemistry was necessary to predict the features of temperature and concentration profiles. Variable bed void fraction was also necessary to accurately predict pressure drop and temperature and concentration profiles. An accurate initial estimate of the effluent composition and temperature from a two-zone, partial equilibrium model was essential for this highly nonlinear problem.

Acknowledgment

This work was sponsored principally by the U. S. Dept. of Energy/Morgantown Energy Technology Center under subcontract from Advanced Fuel Research, Inc., East Hartford, CT. (Contract No. DE-AC21-86MC23075, Richard Johnson, project officer) and also in part by the Advanced Combustion Engineering Research Center at Brigham Young University. Funds for this Center are received from the National Science Foundation (Tapan Mukherjee, project officer), the State of Utah, 25 industrial participants, and the U. S. Department of Energy. Consultations with P. R. Solomon and coworkers at Advanced Fuel Research and A. C. Hindmarsh at Lawrence Livermore Laboratory are greatly appreciated.

1 Thimsen, D., Maurer, R. E., Poole, A. R., Pui, D., Liu, B. and Kittleson, D., "Fixed-bed Gasification Research Using U. S. Coals, Volume 1 Program and Facility Description," final report, DOE/ET/10205-1689 (DE85002000), Morgantown Energy Technology Center, Morgantown, West Virginia (1984).

2 Amundson, N. R. and Arri, L. E.: AIChE J., 24, 87 (1978).

3 Yoon, H., Wei, J. and Denn, M. M.: AIChE J., 24, 885 (1978).

4 Desai, P. R. and Wen, C. Y., "Computer Modeling of the MERC Fixed-bed Gasifier," MERC/CR-78/3, U. S. Department of Energy, Morgantown, West Virginia (1978).

5 Stillman, R.: IBM J. Res. Develop., 23, 240 (1979).

6 Kosky, P. G. and Floess, J. K.: Ind. Eng. Chem. Process Des. Dev., 19, 586 (1980).

7 Daniel, K. J., "Transient Model of a Fixed-bed Gasifier," AIChE 88th National Meeting, June (1980).

8 Daniel, K. J. and Shah, R. P., "Evaluation of Scale-up Parameters for an Advanced Air Blown Fixed-bed Gasifier," paper presented at the Joint Power Generation Conference, Phoenix, Arizona, Sep 28-Oct 2 (1980).

9 Cho, Y. S. and Joseph, B.: Ind. Eng. Chem. Process Des. Dev., 20, 314 (1981).

10 Kim, M. and Joseph, B.: Ind. Eng. Chem. Process Des. Dev., 22, 212 (1983).

11 Yu, W. and Denn M. M.: Chemical Engineering Science, 38, 1467 (1983).

12 Earl, W. B. and Islam, K. A.: CHEMCA 85, paper c2b, 289 (1985).

13 Thorsness, C. B. and Kang, S. W., "A General-purpose, Packed-bed Model for Analysis of Underground Coal Gasification Processes," UCID-20731, Lawrence Livermore National Laboratory, University of California, Livermore, California (1986).

14 Bhattacharya, A., Salam, L., Dudukovic, M. P. and Joseph, B.: Ind. Eng. Chem. Process Des. Dev., 25, 988 (1986).

15 Khanna, R. and Seinfeld, J. H.: Advances in Chemical Engineering (J. Wei, J. L. Anderson, K. B. Bischoff, M. M. Denn and J. H Seinfeld, Editors), Vol. 13 p. 113, Academic Press, Inc., New York (1987).

16 Ergun, S.: Chemical Engineering Progress, 48, 89 (1952).

17 Solomon, P. R. and Colket, M. B.: Seventeenth Symposium (International) on Combustion, p. 131, The Combustion Institute, Pittsburgh, Pennsylvania (1979).

18 Solomon, P. R. and Hamblen, D. G.: Chemistry of Coal Conversion (R. H. Schlosberg, Ed.), Chapter 5, Plenum Press, New York (1985).

19 Serio, M. A., Hamblen, D. G., Markham, J. R., Solomon, P. R.: Energy & Fuels, 1, 138 (1987).

20 Solomon, P. R., Hamblen, D. G., Carangelo, R. M., Serio, M. A. and Deshpande, G. V.: Energy & Fuels, 2, 405 (1988).

21 Hindmarsh, A. C.: "ODEPACK, A Systematized Collection of ODE Solvers," in Scientific Computing (R. S. Stepleman, editor), Vol. 1. p. 55, IMACS Transactions on Scientific Computation, North-Holland, Amsterdam (1983).

22 Smoot, L. D. and Smith, P. J., Pulverized-coal Combustion and Gasification (L. D. Smoot and D. T. Pratt, editors), p. 224, Plenum Press, New York (1979).

23 Smoot, L. D. and Smith, P. J., Coal Combustion and Gasification, p. 92, Plenum Press, New York (1985).

24 Walker, P. L., Rusinko, F., and Austin, L. G., Advances in Catalysis (D. D. Eley, P. W. Selwood and P. B. Weisz, Editors), Vol. XI p.134, Academic Press Inc., New York (1959).

25 Laurendeau, N. M.: Prog. Energy Combust. Sci., 4, 221 (1978).

26 Park, K. Y. and Edgar, T. F.: Ind. Eng. Chem. Res., 26, 237 (1987).

27 Wang, S. C. and Wen, C. Y.: AIChE J., 18, 1231 (1972).

28 Gupta, A. S. and Thodos, G.: AIChE J., 9, 751 (1963).

29 Cho, Y. S.: Modeling and Simulation of Lurgi-type Gasifiers, M. S. Thesis, Washington University, Saint Louis, Missouri (1980).

30 Froment, G. F. and Bischoff, K. B., Chemical Reactor Analysis and Design, John Wiley & Sons, New York (1979).

31 Kunii, D. and Smith, J. M.: AIChE J., 6, 71 (1960).

32 Solomon, P. R., Serio, M. A., Hamblen, D. G., Smoot, L. D. and Brewster, S., "Measurement and Modeling of Advanced Coal Conversion Processes," Second Annual Report #523043-24, U. S. Department of Energy, Morgantown Energy Technology Center, Morgantown, West Virginia (October 1, 1987 to September 30, 1988).

33 Bird, R. B., Stewart, W. E. and Lightfoot, E. N., Transport Phenomena, John Wiley & Sons, New York (1960).

34 Stull, D. R. and Prophet, H., JANAF Thermochemical Tables, Second Edition, Nat. Bur. Stand. (1971).

35 Merrick, D.: Fuel, 62, 540 (1983).

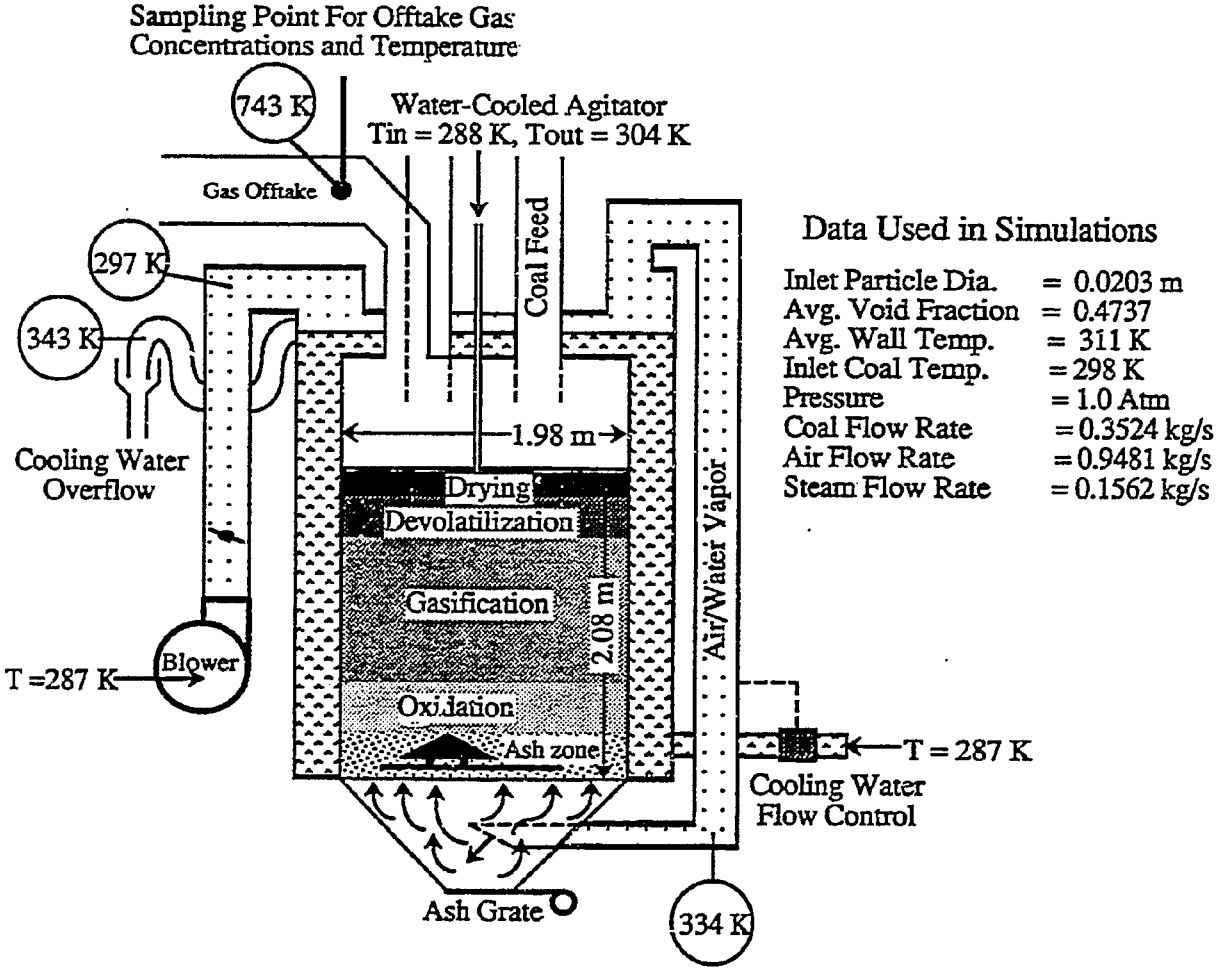

Figure 1. Schematic of typical atmospheric fixed-bed gasifier. Temperatures shown are for gasification of Jetson coal with air. Configuration and data taken from Thimsen et al.[1]

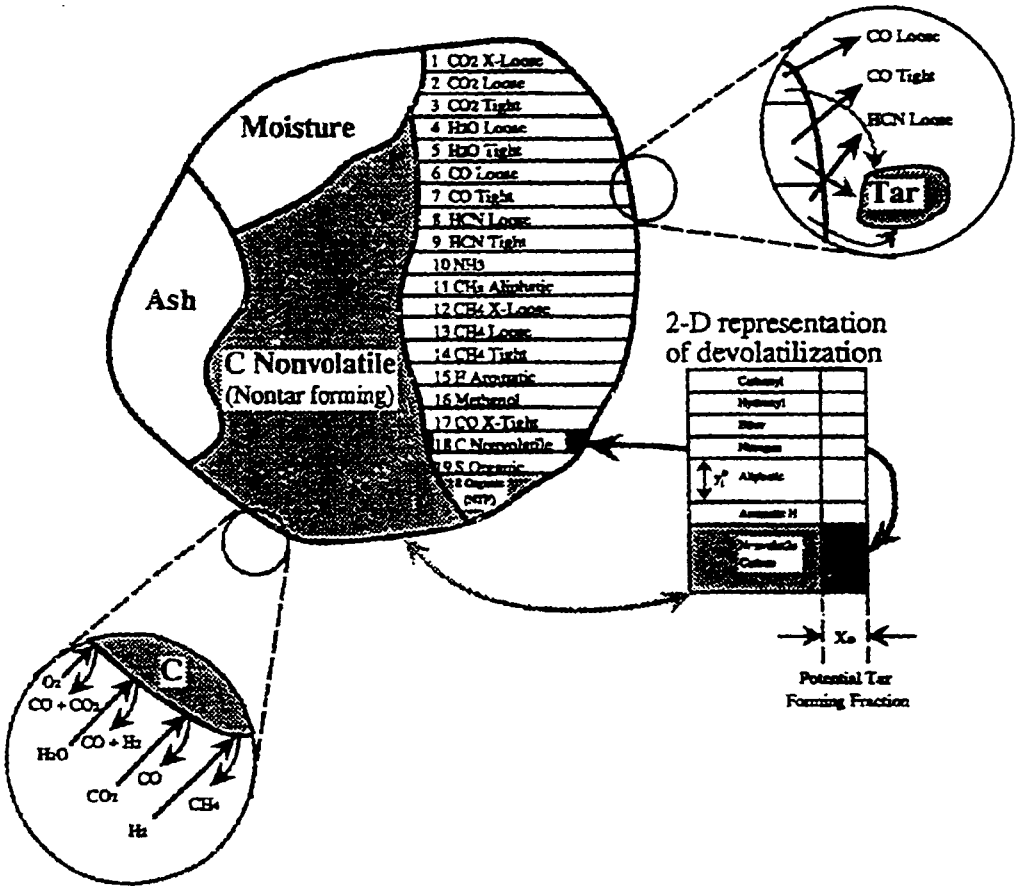

Figure 2. Schematic of coal particle with devolatilization model based on chemical functional groups[17,19]. The potential tar-forming fraction of the nonvolatile carbon functional group evolves as tar. The nontar-forming C and S organic groups evolve via heterogeneous char oxidation or gasification.

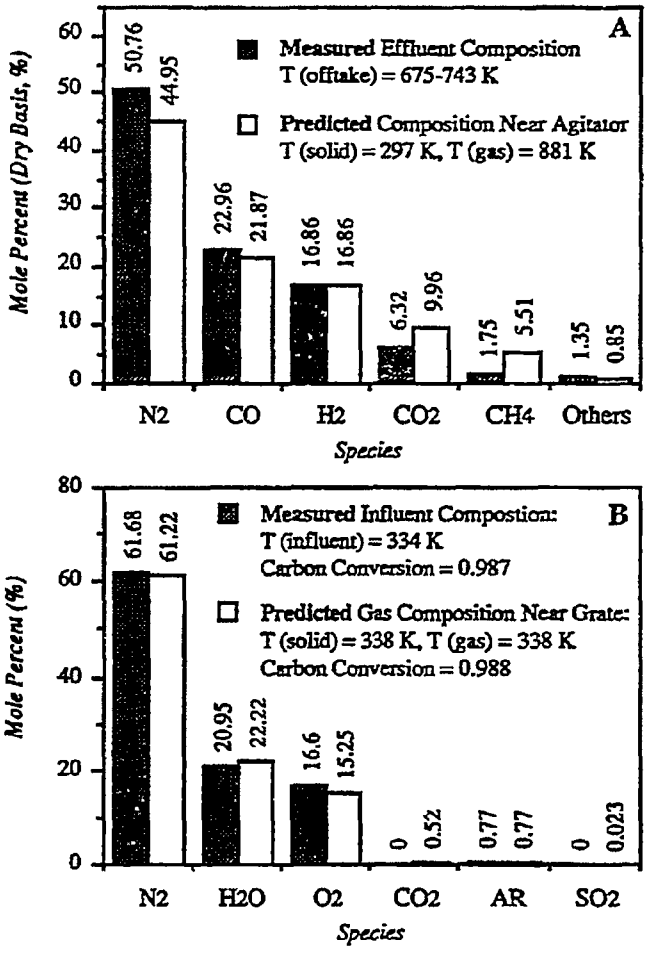

Figure 3. A) Predicted and measured effluent compositions and temperatures, B) predicted and measured influent compositions and temperatures from gasification of Jetson coal in an atmospheric gasifier with air.[1]

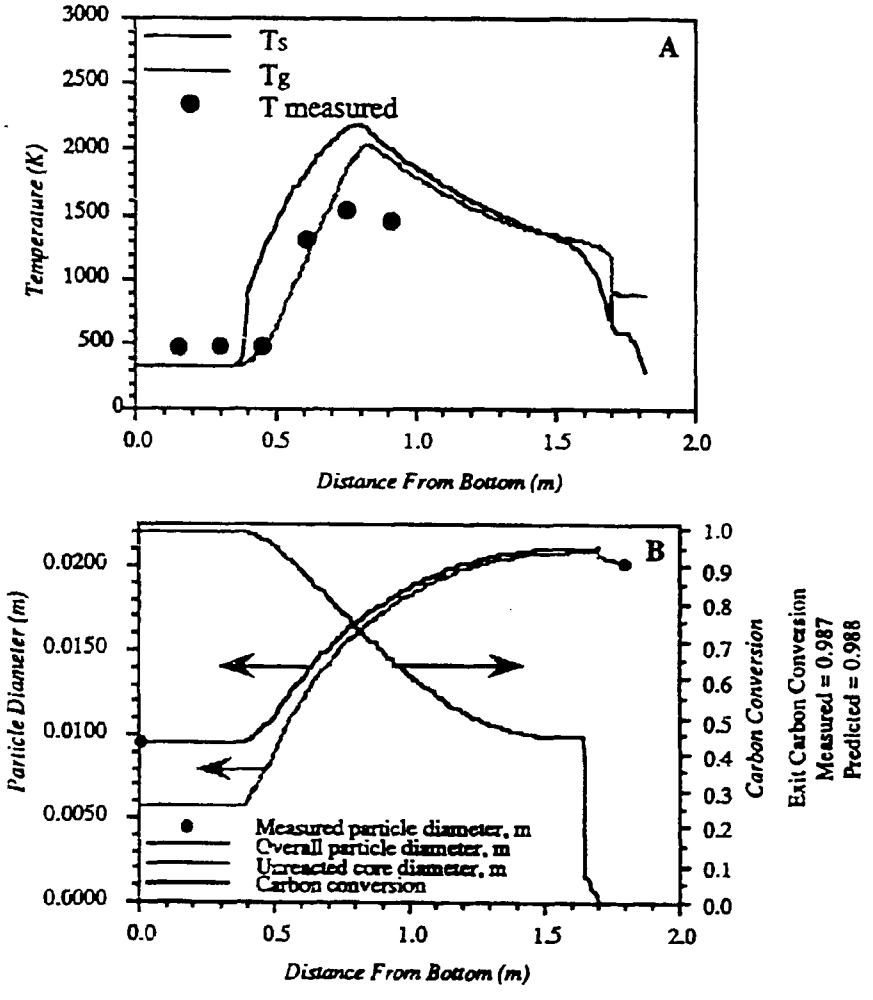

Figure 4. Predicted temperature, carbon conversion, and particle diameter for gasification of Jetson coal in an atmospheric gasifier with air[1]: A) measured and predicted temperature profile, B) predicted carbon conversion, overall and unreacted particle diameter throughout reactor.

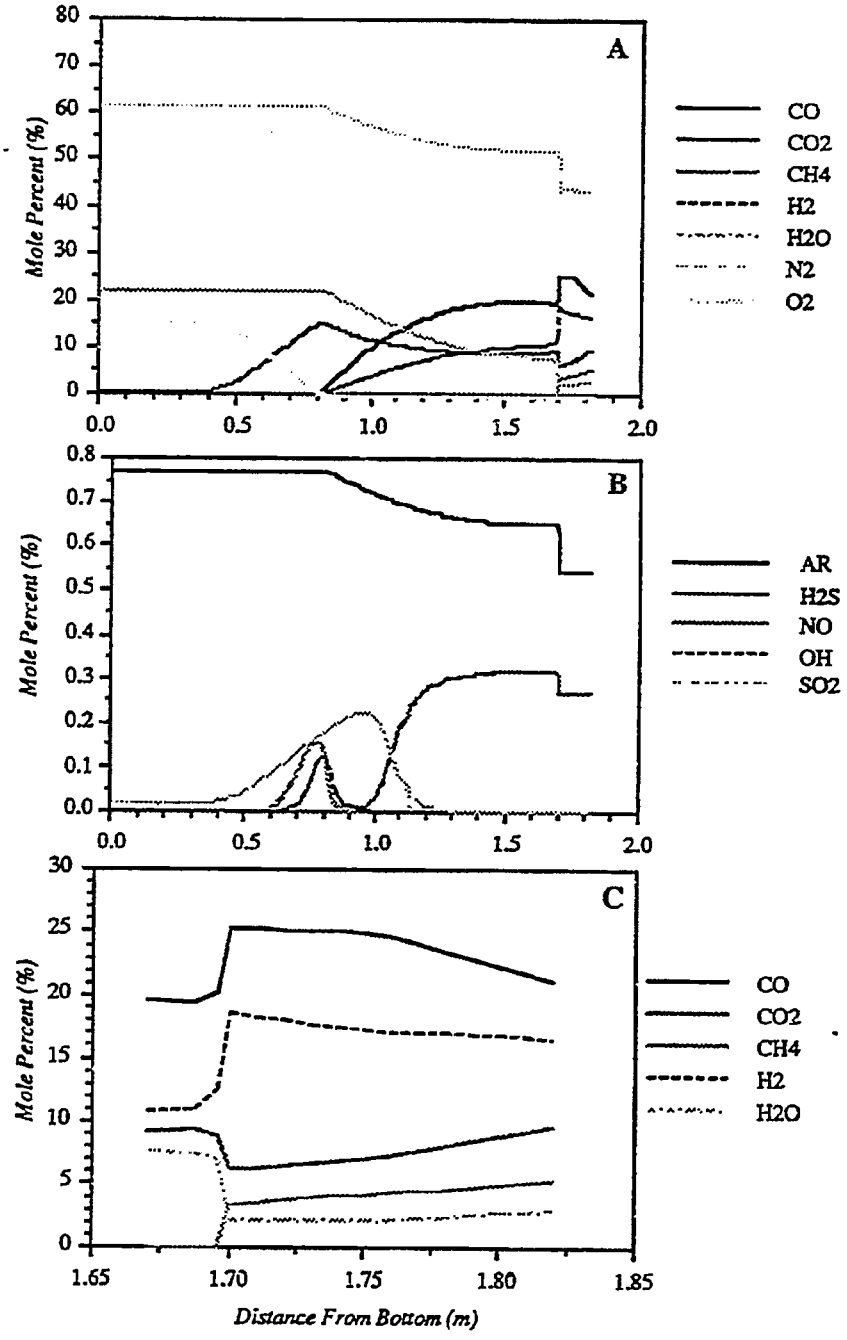

Figure 5. Predicted concentrations for gasification of Jetson coal in an atmospheric gasifier with air: A) major gas species, B) minor gas species, and C) species in devolatilization zone (excluding nitrogen).

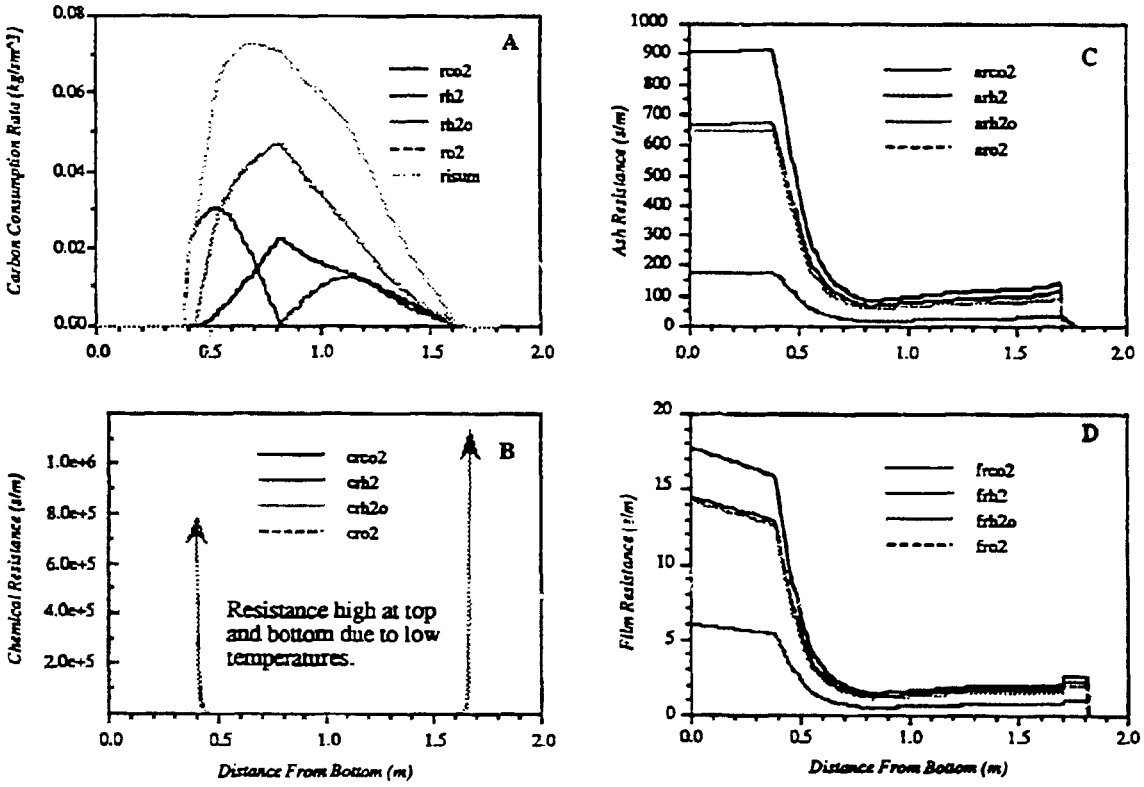

Figure 6. Carbon consumption and resistances for char oxidation and gasification of Jetson coal in an atmospheric fixed-bed gasifier: A) carbon consumption by oxidation and gasification reactions. B) chemical resistance for char oxidation and gasification reactions, C) ash resistance for char oxidation and gasification reactions, D) film resistance form char oxidation and gasification reactions.

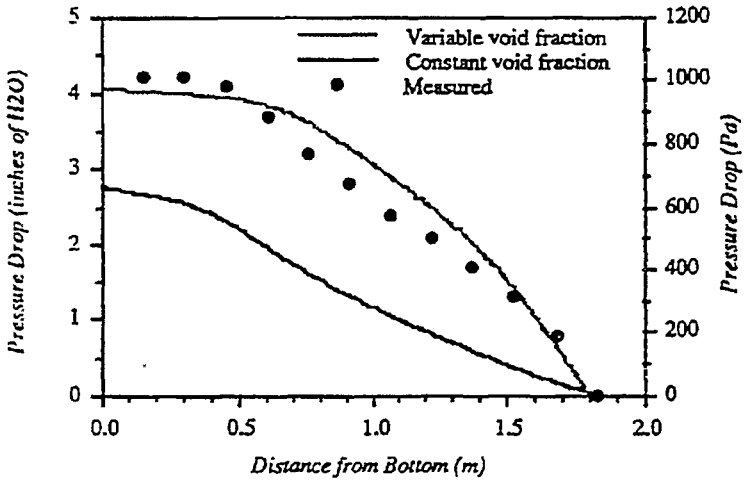

Figure 7. Comparisons of predicted and measured pressure variation in an atmospheric fixed-bed gasifier with (1) constant bed void fraction, 0.47 and (2) variable bed void fraction from 0.31 to 0.64.

Table 1. Assumptions, conservation equations and boundry conditions used in one-dimensional model.

General Assumptions

1. Interdiffusion small compared to chemical reactions.
2. Both particles and gases treated as a continuum.
3. Uniform pressure at control surfaces surrounding particles
4. Negligible viscous heating.
5. Negligible aerodynamic drag.
6. Conduction, radiation and convection to the wall are combined in an effective bulk heat transfer term.
7. Negligible work performed by moving particles.
8. Work due to body forces is small compared to chemical reaction terms.
10. Negligible Soret and Dufour effects.
11. Moving-bed is sufficiently 1-dimensional.
12. Steady state solution will be sought.
13. Negligible axial diffusion.
14. The ideal gas law is valid.
15. Negligible PV-work.
16. Neglibible viscous dissipation.
17. Turbulence effects are implicitly included (See #6).
18. The solid phase internal energy is equal to the solid phase enthalpy.

Equations

Gas & Solid Overall Continuity

$$\begin{cases} \frac{dW_g}{dz} = A\sum_{i=1}^{n} r_i \\ \frac{dW_s}{dz} = -A\sum_{i=1}^{n} r_i \end{cases}$$

Gas & Solid Energy Equation

$$\begin{cases} \frac{dW_g h_g}{dz} = A\left(Q_{sg} - Q_{gw} + \sum_{i=1}^{n} r_i h_{ig}\right) \\ \frac{dW_s h_s}{dz} = A\left(-Q_{sg} - Q_{sw} - \sum_{i=1}^{n} r_i h_{is}\right) \end{cases}$$

Gas Component Continuity

$$\frac{dW_g \omega_{i,g}}{dz} = A\sum_{i=1}^{n} \phi r_i$$

Solid Component Continuity

$$\frac{dW_s \omega_{i,s}}{dz} = -A\sum_{i=1}^{n} \phi r_i$$

Boundary Conditions

- Reactor Top: Solid phase composition and temperature.
- Reactor Bottom: Influent gas composition and temperature.

U.S. DEPARTMENT OF COMMERCE
Technology Administration
National Technical Information Service
Springfield, VA 22161 (703) 605-6000